Nuclear Magnetic Resonance Relaxation Studies of Carbon-13 Labeled Uracil in Transfer Ribonucleic Acid

W. David Hamill, Jr., W. James Horton, and David M. Grant*

Contribution from the Department of Chemistry, University of Utah, Salt Lake City, Utah 84112. *Received January 9, 1980*

Abstract: Unfractionated transfer ribonucleic acid (tRNA) from a uracil requiring auxatrophe of *Salmonella typhimurium* grown in the presence of 90% C-4 carbon-13 labeled uracil is studied by carbon-13 nuclear magnetic resonance spectroscopy (^{13}C NMR). Chemical-shift spectra were obtained at 23.5 kG at five temperatures over a range of 23–82 °C and at 84.6 kG at 37 °C. Spin–lattice relaxation rates were measured at 23.5 kG at four temperatures over a range of 23–60 °C and an approximate relaxation rate was measured at 84.6 kG at 37 °C. Nuclear Overhauser enhancements (NOEs) were measured at 23.5 kG at 37 and at 60 °C. The spectra show two distinct, narrow lines, one at 189.3 ppm readily assignable to 4-thiouridine and the other at 173.7 ppm previously assigned to dihydrouridine. The uridine lines along with lines belonging to ribothymidine and pseudouridine form a band of partially resolved lines about 4.4 ppm wide and centered at 165.1 ppm. This band is the result of the chemical-shift nonequivalence of the uridines, pseudouridines, and ribothymidines caused by the secondary and tertiary structure of the molecule. The relaxation rate data are analyzed in terms of proton dipolar, nitrogen-14 dipolar, and chemical shift anisotropic relaxation mechanisms. The rotational correlation time is computed to be 3×10^{-8} s, which is in agreement with the measurements of others. Changes in the relaxation rates and the NOEs as a function of temperature are discussed in terms of the unfolding of the molecule and in terms of motional freedom of the D loop compared to the rest of the molecule.

Introduction

In recent years nuclear magnetic resonance (NMR) has become a tool of major importance in the structural investigation of transfer RNA (tRNA) in solution. While most of the work to date has been done with ^1H NMR,[1-8] other nuclear probes are beginning to make some interesting contributions to the body of knowledge about tRNA.[9-15]

Specific site labeled carbon-13 probes have recently become important because of the advantages of the large carbon-13 chemical shift range and because with specific site labels a limited number of sites can be examined without interference from overlapping natural abundance lines.[13-15] This laboratory has previously shown the utility of the C-4 carbon-13 labeled uracil as a probe sensitive to its local environment in low molecular weight RNAs.[15,16]

In this report, the C-4 carbon-13 labeled uracil has again been incorporated into the unfractionated tRNAs of *Salmonella typhimurium*. The effects of temperature on tRNA line shape are explored and spin–lattice relaxation rates and nuclear Overhauser enhancements (NOEs) are reported at various temperatures and explained in terms of a dynamical model for the molecule.

Experimental Section

An auxatrope of *Salmonella typhimurium*, JL-1055 (PyrA, PyrG, cdd, udp), requiring arginine, cytidine, and uracil for normal growth, was used for the study.[17] Cells were grown in a homemade 12-L fermentor, using a minimal medium of glucose and salts plus arginine, cytidine, and uracil.[18] The concentration of the carbon-13 labeled uracil in the medium was 5 μg/mL. Ninety percent C-4 carbon-13 labeled uracil was synthesized from 90% carbon-13 labeled potassium cyanide.[19] A total of 384 g of cell paste was grown.

The unfractionated tRNAs were recovered and purified by using a modified procedure of Kelmers et al.[20] followed by the 2-propanol precipitation of Rogg et al.[21] The purity of the product was verified by gel permeation chromatography on Sephadex G-100 Superfine (Pharmacia Fine Chemicals) to be greater than 95%. Residual protein, by the method of Lowry et al.,[22] was determined to be about 0.7%. The DNA content, measured by the method of Gurney and Foster,[23] was less than 0.03%. Methionine acceptance activity, measured by using a modified procedure by Dickman and Boll,[24] was found to average 40 pmol/A_{260} unit compared to an average of 48 pmol/A_{260} unit for *E. coli* tRNA (Sigma Chemical Co.). Carbon-13 isotopic enrichment of the four main bases in tRNA was measured by mass spectroscopy. The uridine was found to be enriched 46 mol % in carbon-13, cytidine was 3 mol % enriched, and adenine and guanosine showed no enrichment. Complete details on the growth and purification procedures are given elsewhere.[18]

Samples for NMR spectroscopy were prepared by dissolving the tRNA in double-distilled H_2O. The resulting solution was 140 mg/mL tRNA, 40 mM $MgCl_2$, 2.2 mM EDTA, and 2 mM dithiothreitol, with 1% dioxane as an internal reference, pH 7.4, self-buffered. Proteinase K (EM Laboratories) was added to some samples to hydrolyze residual nucleases. An aliquot of the sample was analyzed for paramagnetic impurities by means of graphite furnance atomic absorption and found to contain 6.8 ppb copper, 1.4 ppb manganese, and 1.4 ppb iron. Samples for NMR spectroscopy at 23.5 kG were put in a 900-μL Wilmad 529-E-12 cylindrical microcell. The microcell was placed in a 12-mm sample tube containing D_2O. A 250-μL sample for NMR spectroscopy at 84.6 kG was prepared with 10% D_2O for a field frequency lock and placed in a 5-mm sample tube. All glassware was soaked in concentrated nitric

(1) B. R. Reid, L. McCollum, N. S. Ribeiro, J. Abbate, and R. E. Hurd, *Biochemistry*, **18**, 3996 (1979).
(2) R. E. Hurd and B. R. Reid, *Biochemistry*, **18**, 4005 (1979).
(3) R. E. Hurd, E. Azherian, and B. R. Reid, *Biochemistry*, **18**, 4012 (1979).
(4) R. E. Hurd and B. R. Reid, *Biochemistry*, **18**, 4017 (1979).
(5) P. Davanloo, M. Sprinzl, and F. Cramer, *Biochemistry*, **18**, 3189 (1979).
(6) P. Davanloo, M. Sprinzl, K. Watanabe, M. Albani, and H. Kersten, *Nucleic Acids Res.*, **6**, 1571 (1979).
(7) P. H. Bolton and D. R. Kearns, "Biological Magnetic Resonance", Vol. 1, L. J. Berliner annd J. Reuben, Eds., Plenum Press, New York, 1978, p 91.
(8) D. J. Patel, *Annu. Rev. Phys. Chem.*, **29**, 337 (1978).
(9) D. G. Gorenstein and B. A. Luxon, *Biochemistry*, **18**, 3796 (1979).
(10) P. J. M. Salemink, T. Swarthof, and C. W. Hilbers, *Biochemistry*, **18**, 3477 (1979).
(11) R. A. Komoroski and A. Allerhand, *Proc. Natl. Acad. Sci. U.S.A.*, **69**, 1804 (1972).
(12) R. A. Komoroski and A. Allerhand, *Biochemistry*, **13**, 369 (1974).
(13) J. G. Tompson, F. Hayashi, J. V. Paukstelis, R. N. Loeppku, and P. F. Agris, *Biochemistry*, **18**, 2079 (1979).
(14) J. G. Tompson and P. F. Agris, *Nucleic Acids Res.*, **7**, 765 (1979).
(15) W. D. Hamill, Jr., D. M. Grant, W. J. Horton, R. Lundquist, and S. Dickman, *J. Am. Chem. Soc.*, **98**, 1276 (1976).
(16) W. D. Hamill, Jr., D. M. Grant, R. B. Cooper, and S. A. Harmon, *J. Am. Chem. Soc.*, **100**, 633 (1978).
(17) J. Neuhard and J. Ingraham, *J. Bacteriol.*, **95**, 2431 (1968).
(18) W. D. Hamill, Jr., Ph.D. Dissertation, University of Utah, 1977.
(19) W. J. Horton, unpublished work.
(20) A. D. Kelmers, C. W. Hancher, E. F. Phares, and G. D. Novelli, *Methods Enzymol.*, **20**, 3 (1971).
(21) H. Rogg, W. Wehrli, and M. Staehelin, *Biochim. Biophys. Acta*, **195**, 13 (1969).
(22) O. H. Lowry, N. J. Rosebrough, A. L. Farr, and R. J. Randall, *J. Biol. Chem.*, **193**, 265 (1951).
(23) T. Gurney, Jr., and D. N. Foster, *Methods Cell Biol.*, **16**, 45 (1977).
(24) S. R. Dickman and D. J. Boll, *Biochemistry*, **15**, 3925 (1976).

0002-7863/80/1502-5454$01.00/0

acid before use. None of the samples were degassed as dissolved oxygen was not believed to make a significant contribution to carbon relaxation rates greater than 0.5 s^{-1}. A tRNA sample was prepared as above in D_2O to check for intermolecular dipole relaxation.

The 23.5-kG data were measured on a Varian XL-100 NMR spectrometer equipped with a Varian FT module and a Varian 620 f computer. Free induction decays were stored on a Caelus 2.5 × 10^6 word disk. Proton noise decoupling was accomplished with a computer-gated decoupler of our own construction. The observed rf pulses were amplified to give a 16-Ms 90° pulse into a Varian V 4412 probe. Chemical shifts were measured relative to internal *p*-dioxane and converted to parts per million (ppm) from Me_4Si by adding 66.3 ppm to the measured shifts.

The T_1 and NOE data at 23.5 kG were acquired by using the pulse sequence of Mayne et al.[25] (P, τ_1, $\pi/2$, FID_1, P, τ_2, FID_2, ..., P, τ_m, $\pi/2$, $FID_m)_n$ where P is the preparatory procedure, τ_m is the *m*th delay time, $\pi/2$ is a carbon-13 90° pulse, FID_m is the *m*th free induction decay, and *n* is the total number of data aquisitions for each FID. For an inversion recovery T_1 measurement, P is a five T_1 delay followed by a 180° carbon-13 pulse. For a NOE measurement, P is the sequence: decoupler gated off, a five T_1 delay, and the decoupler gated on. A 5000-Hz spectral window was used for all mesurements.

High-field data were taken on the 84.6-kG Bruker HXS-360 superconducting NMR spectrometer at Stanford Magnetic Resonance Laboratory, Palo Alto, Calif., using a 12000-Hz spectral window. A three-point T_1 was measured on this spectrometer, using progressive saturation. All spectra were proton noise decoupled.

With the exception of the T_1 measured at 84.6 kG, all T_1 and NOE measurements were made with 10–12 delay times. The T_1 and NOE values were computed by using a Newton's method fitting algorithm.[25,26] The T_1 data were fitted by using the equation

$$S_i = S_\infty(1 - Ae^{-\tau_i/T_1}) \quad (1)$$

where S_i is the line intensity at delay time τ_i, S_∞ is the line intensity at $\tau_i = \infty$, and A is a parameter that equals 2 for an ideal inversion recovery experiment. The equation

$$S_i = S_0[(1 + \eta(1 - e^{-\tau_i/T_1}))] \quad (2)$$

was used to compute the measured NOE values where S_0 is the line intensity with no NOE and η is the usual NOE parameter (max $\eta = 2$). On lines with both T_1 and NOE data eq 1 and 2 were fit simultaneously, giving a five-parameter fit.

Theoretical Considerations

Spin–lattice relaxation rates ($1/T_1$) of carbon-13 nuclei are the sum of various relaxation mechanisms.[27,28] The most important of these mechanisms for a nonprotonated carbon in a biomolecule such as the C-4 carbon of uracil in tRNA can be shown to be proton dipolar, nitrogen-14 dipolar, and chemical shift anisotropy relaxation.[18,29–31] If isotropic rigid rotor reorientation is assumed and cross correlation neglected, the following equations describe these modes of relaxation.[27,28,32]

$$\frac{1}{T_{1D}} = \frac{1}{15}\frac{h^2\gamma_C^2\gamma_1^2}{r_{CI}^6}S_I(S_I + 1)\chi_I \quad (3)$$

$$\chi_I = J(\omega_I - \omega_C) + 3J(\omega_C) + 6J(\omega_I + \omega_C) \quad (4)$$

$$J(\omega) = \frac{2\tau_R}{1 + \omega^2\tau_R^2} \quad (5)$$

$$\frac{1}{T_{1SA}} = \frac{1}{15}\gamma_C^2H_0^2\Delta\sigma^2J(\omega_C) \quad (6)$$

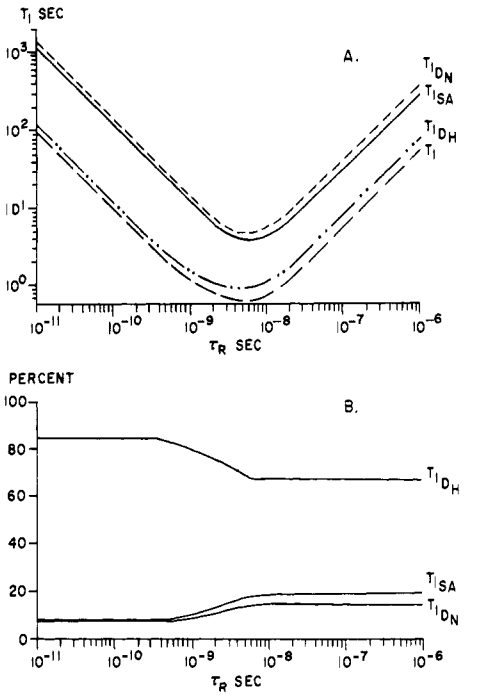

Figure 1. (A) Plot of T_{1DH}, T_{1DN}, T_{1SA}, and the net T_1 vs. τ_R at 23.5 kG. (B) Plot of the percentage contributions of T_{1DH}, T_{1DN}, and T_{1SA} to the net T_1.

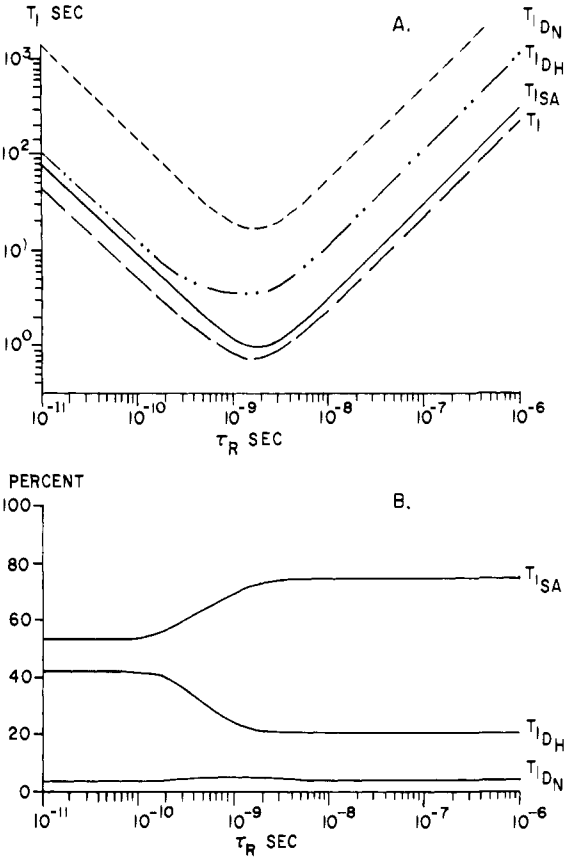

Figure 2. (A) Plot of T_{1DH}, T_{1DN}, T_{1SA}, and the net T_1 vs. τ_R at 84.6 kG. (B) Plot of the percentage contributions of T_{1DH}, T_{1DN}, and T_{1SA} to the net T_1.

Using literature values of uracil bond lengths, bond angles,[33] $\Delta\sigma$,[18] and the equations given above, one can plot the expected contributions of the main relaxation mechanisms (proton dipolar, nitrogen-14 dipolar, and chemical shift anisotropy) to the total

(25) C. L. Mayne, D. W. Alderman, and D. M. Grant, *J. Chem. Phys.*, **63**, 2514 (1975).
(26) C. L. Mayne, Ph.D. Dissertation, University of Utah, 1976.
(27) A. Abragam, "The Principles of Nuclear Magnetism", Oxford University Press, London, 1961, Chapter VIII.
(28) J. R. Lyerla, Jr., and D. M. Grant, *MTP Int. Rev. Sci. Phys. Chem., Ser. One*, **4**, 155 (1972).
(29) R. S. Norton and A. Allerhand, *J. Am. Chem. Soc.*, **98**, 1007 (1976).
(30) A. Allerhand, D. Doddrell, and R. Komoroski, *J. Chem. Phys.*, **55**, 189 (1971).
(31) R. S. Norton, A. O. Clouse, R. Addleman, and A. Allerhand, *J. Am. Chem. Soc.*, **99**, 79 (1977).
(32) T. C. Farrar and E. D. Becker, "Pulse and Fourier Transform NMR", Academic Press, New York, 1971, Chapter 4.
(33) R. F. Stewart and L. H. Jensen, *Acta Crystallogr.*, **23**, 1102 (1967).

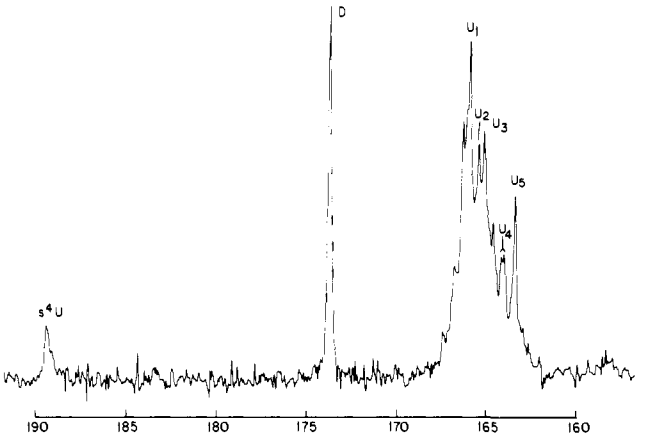

Figure 3. ^{13}C NMR spectrum at 23.5 kG at 37 °C of the C-4 uridine and uridine derivative region of tRNA from *Salmonella typhimurium* cells grown in the presence of C-4 carbon-13 labeled uracil. Parmeters are 5000-Hz spectral window, 61 000 transients, and 1-s cycle time. Line numbers correspond to chemical shifts listed in Table I.

Table I. Chemical Shifts of the C-4 Carbon in Uridine and Uridine Derivatives in tRNA[a]

23.5 kG		84.6 kG	
line	shift	line	shift
s^4U	189.3		
D	173.7	1(D)	173.7
		2(U)	166.8
		3(U)	166.4
		4(U)	166.2
U-1	166.0	5(U)	166.0
U-2	165.5	6(U)	165.5
		7(U)	165.4
U-3	165.2	8(U)	165.2
		9(U)	164.7
U-4	164.2[b]	10(U)	164.3
		11(U)	164.1
U-5	163.5	12(U)	163.5

[a] Chemical shifts were measured at 37 °C relative to internal dioxane and converted to parts per million downfield from Me_4Si by adding 66.3 ppm to each shift. [b] The reported chemical shift is the average of the two lines in Figure 3.

relaxation of the uracil C-4 carbon as a function of the correlation time, τ_R. These plots are shown for a moderate field of 23.5 kG (Figure 1) and for a high field of 84.6 kG (Figure 2).

Nuclear Overhauser enhancements (NOEs) have long been used to indicate the contribution of dipolar relaxation to the total relaxation of the nucleus under observation when the molecule of interest is small and tumbling in the region of extreme narrowing ($\tau_R^2\omega^2 \ll 1$).[34] For molecules such as tRNA which tumble outside the region of extreme narrowing, NOEs are not indicators of the relative contribution of dipolar relaxation, but they can be indicators of rapid segmental motion.[35] One limitation in the usefulness of relaxation rate and NOE measurements in assessing the amount of segmental motion is that, when $\tau_R\omega > 0.3$, the dipolar rates and NOEs are dominated by the more efficient reorientational motion available, be it overall or segmental.[35]

Results

The C-4 uridine region of the ^{13}C NMR spectrum of tRNA at 23.5 kG and at 37 °C is shown in Figure 3. The chemical shifts of the prominent lines are listed in Table I. This spectrum is similar to the one reported earlier except that the downfield line at 189.3 ppm was not visible in the previously reported spectrum.[15] At 84.6 kG the uridine band is spread out (Figure 4) and additional lines are exposed. The chemical shifts of the

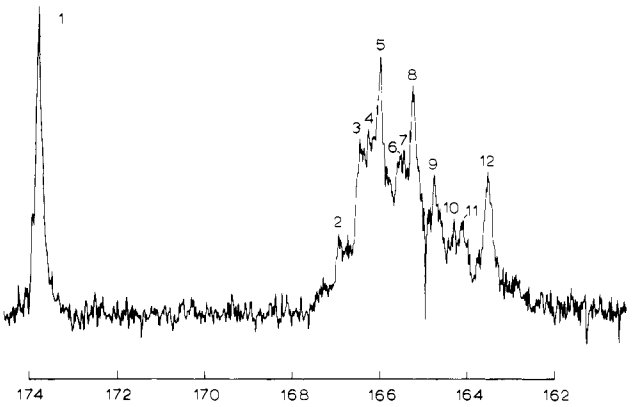

Figure 4. ^{13}C NMR spectrum at 84.6 kG at 37 °C of the C-4 uridine and uridine derivative region of tRNA. Parameters are 12 000-Hz spectral window, 0.68-s cycle time, and approximately 150 000 transients. Line numbers correspond to chemical shifts listed in Table I.

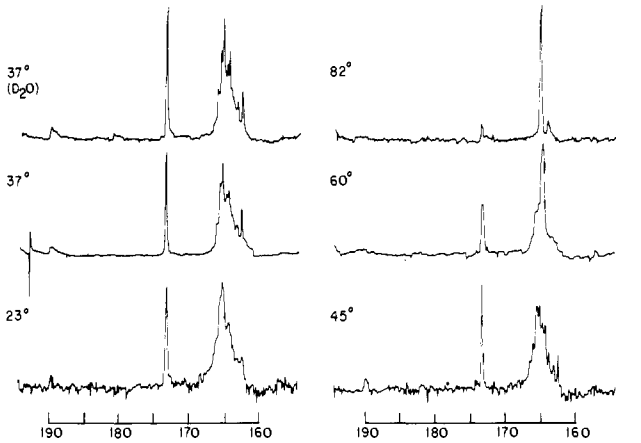

Figure 5. ^{13}C NMR spectra at 23.5 kG of tRNA at various temperatures. Parameters are 5000-Hz spectral width, 10 000 transients for the 23 °C spectrum, 9000 transients for the 37 °C spectrum in H_2O, 2000 transients for the 82 °C spectrum, and about 3500–4000 transients for the remaining spectra.

Table II. Chemical Shifts of the C-4 Carbons in Uridine Nucleosides[a]

nucleoside	shift	nucleoside	shift
4-thiouridine	190.9	uridine	165.8
dihydrouridine	173.5	pseudouridine	165.0
thymidine	166.0		

[a] Chemcial shifts were measured in water relative to internal dioxane and converted to parts per million from Me_4Si.

uridine lines in Figure 4 are also listed in Table I. The effects of temperature on chemical shifts and line shape at 23.5 kG are shown in Figure 5.

Assignment of some of the lines in Figure 3 was made by comparison with the C-4 chemical shifts of the common uridine derivatives found in tRNA (Table II). The line at 189.3 ppm is readily assigned to 4-thiouridine. The line at 173.7 ppm has previously been assigned to dihydrouridine.[15] The lines between 163.0 and 167.5 ppm are primarily uridine lines experiencing different local magnetic environments. These differing environments are presumably due to ring current shifts from adjacent bases whose relatively fixed positions are imposed by the ordering effect of the secondary and tertiary structure of tRNA. In contrast to the broad uridine lines is the relatively narrow dihydrouridine line. The narrowness of this line suggests the absence of rigidly ordered structure in the D loop. Two other minor uridine components present in sufficient quantity to be seen are pseudouridine and ribothymidine.[36] As seen in Table II the C-4 carbon shifts

(34) D. Doddrell, V. Glushko, and A. Allerhand, *J. Chem. Phys.*, **56**, 3683 (1972).

(35) J. J. Led, D. M. Grant, W. J. Horton, F. Sundby, and K. Vilhelmsen, *J. Am. Chem. Soc.*, **97**, 5997 (1975).

(36) B. G. Barrell and B. F. C. Clark, "Handbood of Nucleic Acid Sequences", Joynson-Bruvvers, Oxford, 1974.

Table III. Relaxation Rates of C-4 Carbon Lines in Uridine and Uridine Derivatives in tRNA[a]

conditions	s^4U[b] (189.3)	D (173.7)	U (166.0)	U_2 (165.5)	U_3 (165.2)	U_4 (164.2)	U_5 (163.5)
23 °C in H_2O	*c*	0.50 ± 0.05	0.40 ± 0.03	*d*	*d*	*d*	*d*
37 °C in H_2O	0.7 ± 0.2	0.59 ± 0.04	0.63 ± 0.04	0.59 ± 0.04	0.63 ± 0.04	0.67 ± 0.09	0.63 ± 0.06
37 °C in D_2O	0.7 ± 0.3[e]	0.45 ± 0.04	0.34 ± 0.02	0.32 ± 0.04	0.33 ± 0.02	0.3 ± 0.1	0.34 ± 0.05
45 °C in H_2O	*c*	0.56 ± 0.03	0.71 ± 0.05	0.67 ± 0.04	0.63 ± 0.04	0.67 ± 0.04	0.7 ± 0.1
60 °C in H_2O	*c*	0.40 ± 0.03	0.67 ± 0.04	*d*	0.53 ± 0.03	0.7 ± 0.1	0.7 ± 0.1
37 °C HXS-360[f]	*c*	0.5 ± 0.3	0.3 ± 0.2				

[a] Relaxation rates are in s^{-1} with 1σ standard deviations based on data scatter. True error bars are considered to be ±25% or less unless otherwise indicated. [b] Chemcial shifts are from Table I. [c] Signal to noise of 4-thiouridine line not adequate for relaxation rate measurement. [d] Line not resolved. [e] Relaxation rate measured by progressive saturation. [f] Relaxation rate measured by a three-point progressive saturation experiment.

Table IV. η's of C-4 Carbon Lines in Uridine and Uridine Derivatives in tRNA

conditions	s^4U[a] (189.3)	D (173.7)	U_1 (166.0)	U_2 (165.5)	U_3 (165.2)	U_4 (164.2)	U_5 (163.5)
37 °C in H_2O	*b*	0.2 ± 0.3	0.3 ± 0.2	0.3 ± 0.2	0.3 ± 0.2	0.4 ± 0.3	0.4 ± 0.3
37 °C in D_2O	0.4 ± 0.5	0.5 ± 0.1	0.1 ± 0.1	0.1 ± 0.1	0.1 ± 0.1	0.0 ± 0.2	0.1 ± 0.1
60 °C in H_2O	*b*	1.0 ± 0.2	0.3 ± 0.2	*c*	0.5 ± 0.1	0.5 ± 0.3	0.4 ± 0.3

[a] Chemical shifts are from Table I for tRNA at 37 °C in H_2O. [b] Signal to noise for 4-thiouridine not adequate for NOE measurement. [c] Line not resolved.

of these two nucleosides are too close to the C-4 carbon shifts of uridine to be distinguished in the tRNA NMR spectrum. Assignments of the pseudouridine and ribothymidine lines along with the respective uridine lines will have to await the purification and ^{13}C NMR analysis of a single tRNA species.

Integration was performed on the spectra taken for 23.5 kG at 37 and 82 °C, and for 84.6 kG at 37 °C. At 23.5 kG and 37 °C, 4-thiouridine comprised 3% of the total integral, dihydrouridine 14%, and the uridine band 83%. These results are within experimental error of the calculated percentage contributions for *E. coli* tRNA of 5% for 4-thiouridine, 13% for dihydrouridine, and 82% for the combined uridine, pseudouridine, and ribothymidine nucleosides. At 86.4 kG and 37 °C the integrated intensities were 14% for dihydrouridine and 86% for the uridine band (spectral window not set for observation of 4-thiouridine). These values are also within experimental error, especially when corrected for a contribution of 3–5% for 4-thiouridine, of the estimated values. At 82 °C and 23.5 kG, 4-thiouridine was not observed, and the intensities were 11% for dihydrouridine, 75% for the uridine line (72% expected), and 14% for the upfield line assigned to pseudouridine (11% expected). The positive deviation of the pseudouridine integral is an instrumental artifact due to its proximity to the large uridine line. Again there is excellent agreement with expected values indicating no observable contamination by other nucleic acids and very little loss by C–N bond cleavage.

Measured relaxation rates at 23.5 kG for various temperatures and at 84.5 kG for 37 °C are listed in Table III. Measured values of η at 23.5 kG are listed in Table IV. As an aid in the discussion of the relaxation data presented in Table III, effective rotational correlation times (τ_R's) were computed for these data by using eq 3–6 and assuming rigid rotor isotropic reorientation. Literature values for bond angles and bond lengths were used for uracil[33] and dihydrouracil.[37] Values used for $\Delta\sigma$ are 160 ppm for the C-4 carbon in uracil[18] and 220 ppm for the C-4 carbon in dihydrouracil.[38] As is apparent from Figures 1 and 2, two τ_R's can be computed for each relaxation rate. One τ_R represents motion outside the limit of motional narrowing (slow motion) and the other τ_R represents motion in the limit of motional narrowing (fast motion). The computed τ_R's for motion outside the limit of extreme narrowing corresponding to the relaxation rates tabulated in Table III are listed in Table V.

Table V. "Slow" Correlation Times (τ_R's) for the Uridines and Dihydrouridones in tRNA[a]

conditions	D	U_1	U_2	U_3	U_4	U_5
23 °C in H_2O	54 ± 6	44 ± 4	*b*	*b*	*b*	40 ± 6
37 °C in H_2O	45 ± 3	27 ± 2	29 ± 2	27 ± 2	26 ± 4	27 ± 4
37 °C in D_2O	44 ± 4	31 ± 3	33 ± 5	32 ± 3	30 ± 10	31 ± 5
45 °C in H_2O	48 ± 3	24 ± 2	26 ± 2	27 ± 2	26 ± 2	24 ± 4
60 °C in H_2O	68 ± 6	26 ± 6	*b*	33 ± 2	26 ± 6	26 ± 6
37 °C HXS-360	16 ± 10	13 ± 10	*c*	*c*	*c*	*c*

[a] Correlation times (τ_R's) are in nanoseconds. Error bars are calculated from error bars listed in Table IV. [b] Line not resolved. [c] T_1 of line not measured.

Discussion

It is recognized that at high concentrations tRNA tends to form aggregates, particularly in the presence of high salt.[11,39] Komoroski and Allerhand performed their relaxation rate studies at a tRNA concentration of 200 mg/mL.[11] They also demonstrated that their sample was more highly aggregated than one with a tRNA concentration of 80 mg/mL. Since the sample concentration used in this report is 140 mg/mL or midway between the concentrations reported by these earlier workers, the effects of aggregation are expected to be somewhat less than that experienced with the 200 mg/mL sample. Although a more detailed discussion is given below, it is worth noting here that, like Komoroski and Allerhand,[11] we see no sudden changes in τ_R that would indicate a breaking up of aggregation while increasing the temperature up to 60 °C. These data suggest in low salt solutions that the aggregates, if they exist, are very weak and transitory in nature. This situation contrasts to that at 1.0 M NaCl, where tRNA forms very tight aggregates.[39]

The reorientation time for tRNA at 37 °C was found to be 3×10^{-8} s (Table V), in agreement with the measurements of others.[9,11,40] At 23 °C there is a 33% decrease in the uridine C-4 carbon relaxation rate. This change is apparently due to increasing solvent viscosity and increased aggregation of the tRNA molecules.[11] The increased aggregation is also obvious from the broadening of the uridine lines at this temperature (Figure 5).

At 37 °C a 47% decrease is seen in the uridine relaxation rate in going from an H_2O solvent system to a D_2O solvent system. Forty percent of this change can be accounted for by the loss of the proton at N-3. The change in the relaxation rate for the dihydrouridines is considerably less because of the presence of the two protons at C-5. The uracil correlation times show an average increase of 15%. Solvent isotope viscosity effects in D_2O have been shown to cause a 10% increase in the correlation time

(37) D. Rohrer and M. Sundaralingam, *Chem. Commun.*, 746 (1968).
(38) G. C. Levy and U. Edlund, *J. Am. Chem. Soc.*, **97**, 5031 (1975).
(39) I. C. P. Smith, T. Vamane, and R. G. Shulman, *Science*, **159**, 1360 (1968).
(40) M. Ehrenberg, R. Rigler, and W. Wintermeyer, *Biochemistry*, **18**, 4588 (1979).

for sucrose[30] and most likely are the explanation for the observed change in the tRNA correlation times (Table V). The ability of the proposed model to account for the change in the relaxation rates upon a change of solvent also demonstrates that intermolecular dipolar relaxation is not contributing to the relaxation of the uridine C-4 carbons in tRNA. The values of η for the uridine lines at this temperature are within experimental error of the theoretical minimum of 0.15 for a body tumbling outside the limit of motional narrowing.[34,35] The decrease in η upon changing to D_2O is an indication of the decrease in the importance of dipolar relaxation in the C-4 uridine carbons. There is no readily apparent explanation for the increase in η for dihydrouridine upon changing to a D_2O solvent. If the true value in both H_2O and D_2O were about 0.5, then one could cite this as evidence, along with the narrow line shape, of the presence of segmental motion in excess of that experienced by the uridines.[35]

A comparison of the calculated τ_R values for the uridines with those of the dihydrouridines at all temperatures shows a 40% lower rate of reorientation for the dihydrouridines. The narrow dihydrouridine line, as pointed out above, and the slightly higher η values for this nucleoside both suggest that the lower than expected relaxation rates for this moiety are due to the presence of a greater amount of segmental motion in the D loop than experienced by the uridines in the rest of the molecule. At 84.6 kG the uridine relaxation rate is seen to decrease by 47%. According to eq 3-6 this change should have been about 80% for a molecule tumbling outside the limit of motional narrowing. This discrepancy, also reflected in Table V, must be more fully documented with more accurate relaxation rate measurements at the higher field before any attempt can be made to reconcile the differences. The significance of the high field relaxation rate measurement, albeit somewhat approximate, is that the results validate the model used to analyze the data.

As the sample temperature is raised from 37 to 45 and then to 60 °C, with the exception of U-3, little change is seen in the uridine relaxation rates and η's. The dihydrouridine relaxation rates and η's generally follow the uridine values up to 45 °C. At 60 °C, however, the dihydrouridine relaxation rate decreases from 0.56 to 0.40 s^{-1} (a 29% decrease) and η goes from 0.2 to 1.0. While the calculated slow τ_R's indicate a 42% increase in the correlation time for this moiety, the increase in η clearly demonstrates that at 60 °C there has been a significant increase in the motional freedom for the dihydrouridines. The dramatic change in the uridine band shape (Figure 5) at 60 °C along with the small but significant decrease in the relaxation rate of the U-3 line and similar increase in its η are further indication that collapse of the tRNA has begun. These data suggest some of the details of melting: that the D and TΨC loops have broken apart and that some of the secondary structure involving base pairs may have been lost. The uridine relaxation rates and η's suggest, however, that considerable secondary structure remains, presumably held together by the base pairs in the stems which are partially holding the molecule together and preventing totally random coil type reorientation from dominating the uridine relaxation rates.

Acknowledgments. This work was presented at the 8th International Conference on Magnetic Resonance in Biological Systems, Nara, Japan, Sept 1978. This work was supported in part by the U.S. Public Health Service through the National Institutes of Health under Awards GM08521 and RR00574. The synthesis of the carbon-13 labeled uracil was supported by ERDA Award E(11-1)-2451. The authors are indebted to the Stanford Magnetic Resonance Laboratory supported by National Science Foundation Award GP23633 and National Institutes of Health Award RR00711 and to Dr. Woody Conover for the 84.5-kG data. One of the authors (W.D.H.) is indebted to the National Science Foundation for support in the form of a Predoctoral Fellowship and to the National Institutes of Health for Postdoctoral Fellowship GM05546. The authors also wish to thank Dr. James McClosky for the mass spectroscopic analysis and Dr. John Ingraham for supplying the *Salmonella typrimurium* JL-1055 culture.

Thermally and Photochemically Initiated Polymerization Processes in the Solid State

Jeremy K. Burdett[1]

Contribution from the Department of Chemistry, The University of Chicago, Chicago, Illinois 60637. *Received February 5, 1980*

Abstract: A simple method, which allows the calculation for solid-state structures of the molecular orbital structure of a fragment within the solid, is described. The resulting orbitals, a subset of the crystal orbitals, allow study of the way an isolated molecular fragment is attached to its solid-state environment. The derivation of correlation diagrams which relate the orbitals of a monomeric unit to those of the same fragment bound into an infinitely repeating polymer allows comment on whether such a polymerization process is thermally or photochemically allowed. For two specific examples, those of $S_2N_2 + \Delta \rightarrow (SN)_x$ and $RC{\equiv}CC{\equiv}CR + h\nu \rightarrow (RCC{\equiv}CC(R){=})_x$, thermally and photochemically allowed processes, respectively, are found.

Introduction

The Woodward-Hoffmann rules[2] and their associated molecular orbital background in terms of orbital symmetry conservation are now well established in organic chemistry. Their use often allows ready prediction of the experimental conditions, thermal or photochemical, for successful generation of desired products. Whether or not polymerization reactions in condensed media are amenable to a similar treatment has not been tackled in an analogous way. This is due, in part at least, to the fact that, whereas the molecular orbitals of the monomeric species are readily derived, the orbitals of the polymeric products are defined in terms of the Bloch functions which take into account the infinite but periodically repeating nature of the "molecule" and are usually represented as the electronic band structure of the solid.[3] In this

(1) Fellow of the Alfred P. Sloan Foundation and Henry and Camille Dreyfus Teacher-Scholar.

(2) Hoffmann, R.; Woodward, R. B. "The Conservation of Orbital Symmetry"; Verlag Chemie: Weinheim/Bergstr., West Germany, 1970.

(3) See, for example, Stiddard, M. B. H. "The Elementary Language of Solid State Physics"; Academic Press: New York, 1975.

0002-7863/80/1502-5458$01.00/0